

Heat Transfer Correlation for Anti-icing Systems

J. M. Brown,* S. Raghunathan,† and J. K. Watterson‡

Queen's University of Belfast, Belfast, Northern Ireland BT9 5AG, United Kingdom
and

A. J. Linton§ and D. Riordon¶

Bombardier Aerospace Shorts, Belfast, Northern Ireland BT3 9DZ, United Kingdom

Experimental investigations directed toward further understanding and improved prediction of heat transfer in an aircraft nacelle anti-icing system are presented. The results are correlated with existing predictions. A unique correlation based on the heat transfer impingement area is developed. The correlation is independent of the distance between the jet and the impingement surface and the distance between the jets.

Nomenclature

A_{imp}	=	total area of jet impingement
a, b, c	=	constants
C	=	constant
C_p	=	specific heat capacity of air
C_x	=	distance between the holes
d	=	hole diameter
G	=	mass flow per unit area of impingement
h	=	heat transfer coefficient
\bar{h}	=	average heat transfer coefficient, $q/A_{\text{imp}}(T_{\text{piccolo}} - \bar{T}_{\text{lipskin}})$
L	=	length of nozzle
N	=	number of holes
Nu	=	local Nusselt number
\bar{Nu}	=	average Nusselt number
Pr	=	Prandtl number
q	=	heat transfer from impinging air, $w \times C_p \times (T_{\text{piccolo}} - \bar{T}_{\text{exhaust}}) \times 3600$
Re	=	Reynolds number based on hole diameter, $(w/N_{\text{holes}}) \times (d/A_{\text{hole}}\mu)$
Re_G	=	Reynolds number based on impingement area, $4Gd/\pi\mu$
T	=	temperature
\bar{T}	=	average temperature
w	=	mass flow rate
Zn	=	perpendicular distance from hole to lipskin
θ	=	jet impingement angle
μ	=	dynamic viscosity

Introduction

INGESTION of ice formed and shed from the internal surface of a jet engine intake often leads to engine damage and, therefore, is a safety hazard for aircraft in flight. To protect aircraft from such a hazard, anti-icing systems (Fig. 1) are employed. A jet engine anti-icing system is housed in the engine nacelle and consists of hot air bled from the compressor and ducted forward to a pipe (Fig. 2)

Received 10 April 2001; revision received 15 August 2001; accepted for publication 17 August 2001. Copyright © 2001 by the American Institute of Aeronautics and Astronautics, Inc. All rights reserved. Copies of this paper may be made for personal or internal use, on condition that the copier pay the \$10.00 per-copy fee to the Copyright Clearance Center, Inc., 222 Rosewood Drive, Danvers, MA 01923; include the code 0021-8669/02 \$10.00 in correspondence with the CCC.

*Research Student, School of Aeronautical Engineering; currently Lead Engineer, Airbus U.K.

†Bombardier Aerospace-Royal Academy Chair and Head of School, School of Aeronautical Engineering, Associate Fellow AIAA.

‡Lecturer, School of Aeronautical Engineering, Member AIAA.

§Staff Technical Engineer, Power Plant and Systems.

¶Head, Power Plant and Systems.

with several small holes known as a piccolo tube. The piccolo tube is designed to run circumferentially around the intake. The hot air jets from the holes impinge on the inner surface of the intake leading edge to melt the ice formed.

There are regulations that define the required performance level of anti-icing systems used in large civil jet aircraft. These regulations are contained in Federal Aviation Regulations and Joint Airworthiness Requirements. The challenge to the aerospace industry is to design a cost-effective anti-icing system that meets these requirements.

The performance of the anti-icing system at a given flight condition depends on several factors. These include the mass flow rate, temperature drop between the engine compressor and piccolo tube, the amount of water catch, the impinging limits on the nacelle surface, and the conditions for thermal equilibrium at the nose cowl surface. A critical aspect in the design of an anti-icing system is the prediction of the heat transfer of the impinging jets from the piccolo tube.

The fluid mechanics and heat transfer of even a single jet impinging on a surface is complex, and therefore, the prediction of heat transfer in such jets has met with only limited success.^{1–3} Generally the heat transfer characteristics of a single jet can be represented as a correlation between average Nusselt number, Reynolds number, and Prandtl number.

Because of the complexities of the flow, it is generally accepted that the prediction of heat transfer in an anti-icing system is not accurate, and the present methods of prediction are conservative.

This paper presents experimental investigations directed toward further understanding and improved prediction of heat transfer in an aircraft nacelle anti-icing system. The results are correlated with existing predictions.

Previous Experimental Research

Gardon and Cobonpue⁴ experimented with both single and multiple jets to measure the heat transfer. Their results suggest that the maximum stagnation point heat transfer for a single jet is obtained with a separation ratio of $Zn/d = 5-7$ between the jet origin and the impingement surface. This has been demonstrated to be approximately equal to the length of the potential core of the jet.^{4–7} In the case of multiple jet arrays impinging on a flat surface, Gardon and Cobonpue⁴ found the optimum separation distance to reduce, which is in agreement with the findings of Huang and El-Genk.⁸ Metzger et al.⁹ investigated multiple jet impingement on a concave surface and found the optimum separation distance to be $3 \leq Zn/d \leq 5$ for $1150 \leq Re \leq 5500$ (Reynolds number based on nozzle diameter and jet exit velocity). This optimum separation distance reduces for higher values of Reynolds number.

Perry¹⁰ and Sparrow and Lovell¹¹ investigated the effect on heat transfer of θ , the jet angle of incidence. Sparrow and Lovell¹¹ used a naphthalene sublimation technique to measure the mass transfer from a plate of solid naphthalene due to impingement of a single air

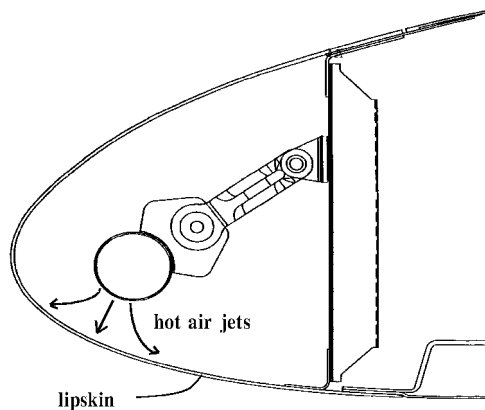


Fig. 1 Piccolo nacelle anti-icing system.

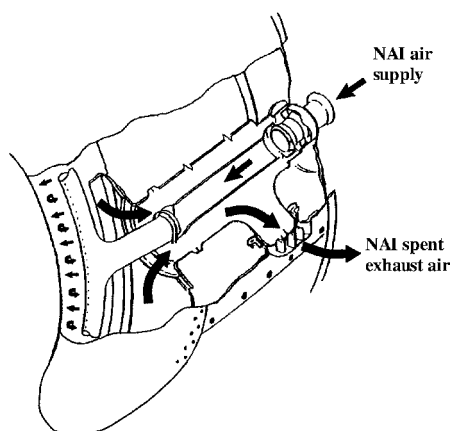


Fig. 2 Nacelle anti-icing exhaust system.

jet, for $30 \leq \theta \leq 90$ deg. The maximum mass transfer was noted for a 90-deg impingement angle, which reduced by 15–20% when the angle was reduced to 30 deg.

Martin¹² shows a direct analogy between mass and heat transfer such that the conclusions of Sparrow and Lovell¹¹ are equally applicable to heat transfer.

The crossflow was investigated by Hollworth and Bowley,¹³ Colin and Olivari,¹⁴ and Sparrow et al.¹⁵ Colin and Olivari¹⁴ concluded that the effects of crossflow are opposite depending on the strength of the jet and whether or not the crossflow is bounded, that is, the deflection caused by an unbounded crossflow is greater than that caused by a crossflow in a bound space, for strong jets, and smaller for weak jets. Hollworth and Bowley¹³ noted that higher values of impingement heat transfer are evident for jets generated using orifices compared to those generated using nozzles. This difference is greater at lower separation distances, suggesting that it is due to the aperture-induced turbulence within the jet because this is less important at higher values of Zn/d (as observed by Gardon and Cobonpue⁴).

The effect of nozzle geometry on heat transfer from a single round jet was investigated by Obot et al.¹⁶ The turbulence and velocity across the nozzle exit and along the centreline of the jet were measured for nozzles with a range of L/d values. Each nozzle was investigated with both a contoured and a sharp-edged inlet. They concluded that for short nozzles, $L/d = 1$, the inlet geometry has a large effect on the velocity profile at the jet exit and the heat transfer (for separation ratios $Zn/d \leq 12$).

The effects of mutual interference of multiple jets¹⁷ and Reynolds number¹⁸ have also been investigated.

Experimental Program

Experiments were performed on a full-scale, two-dimensional model of an anti-icing system installed in a low-speed wind tunnel. The wind tunnel was a closed circuit, continuous flow, atmospheric tunnel with an effective working section of 1.14×0.86 m and a

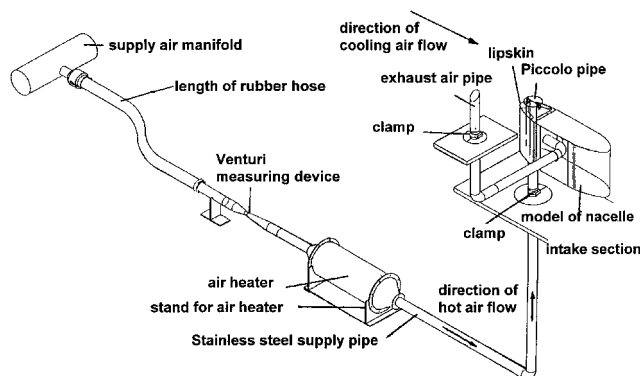


Fig. 3 Experimental setup.

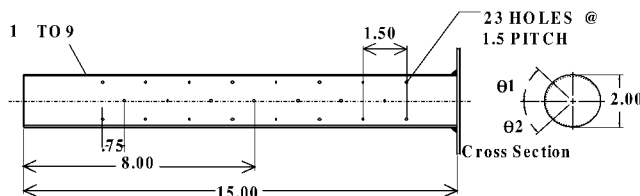


Fig. 4 Geometries of piccolo pipes 1-9.

maximum velocity of 50 m/s, corresponding to a Reynolds number of $3.6 \times 10^6 \text{ m}^{-1}$ (using a characteristic length of 1 m and assuming International Standard Atmosphere conditions at sea level).

The tunnel air temperature was close to ambient during all testing, and the speed of the tunnel was maintained at 40 m/s. The tunnel air temperature was continually monitored, and all tests were carried out at a temperature below 40°C.

The model of the lipskin was a representation of an existing nacelle, which is currently in service on a civil aircraft and was mounted in the wind tunnel on a sting. The model was constructed as a box structure with a D shaped chamber zone on both the front and rear ends. The general arrangement of the setup is shown in Fig. 3. The forward lipskin was constructed from high-temperature aluminium alloy 2219 of 0.064-in. (1.626 mm) thickness and was profiled to represent accurately the geometry of an existing nacelle, which is manufactured by Bombardier Aerospace Shorts. The rear skin was of the same profile as the front lipskin to provide an aerodynamic profile and, therefore, minimize turbulence of the wind-tunnel airflow. Large side plates were attached to the model forward of the front bulkhead. These were to ensure that a two-dimensional flow and, hence, uniform cooling was achieved over the lipskin surface. The endplates were riveted in place with cutouts to allow the piccolo tubes to be inserted. The model was mounted in the wind tunnel on a sting. The sting was bolted to a base, which was attached to the rear bulkhead of the model. An inclinometer was used to ensure that the model was horizontal before each run.

Piccolo pipes were constructed from titanium tubing, 15 in. (38.1 cm) long, 0.028 in. (0.711 mm) thick, with an outside diameter of 2.0 in. (50.8 mm). All of the piccolo tubes had a pattern of holes drilled in three rows with the holes of the middle row staggered to be at the midpoint of the holes on the other two rows. Details of piccolo pipe hole pattern are shown in Fig. 4 and Table 1. The angle between the rows of holes, measured at the center of piccolo pipe, were chosen to keep a constant area of jet impingement on the lipskin surface as the normal distance from the piccolo pipe to the lipskin surface was varied during the experiment. Hot air, after impingement on the lipskin, was exhausted from the D-chamber to the laboratory through a 2-in.-diam (50.8 mm) pipe attached to the back of the front bulkhead.

The heater used for producing hot jets was a Secomak model 15/2. It had a maximum power of 18 kW with a maximum air temperature of 300°C. The heater consisted of three ceramic tubes, each with two resistive wire elements wound along their length. The wiring of the heater was contained in a metal box mounted on the topside of the heater body. The wires were connected to a three-phase thyristor

Table 1 Piccolo pipes

Item no.	Part no.	$\varnothing X$, hole \varnothing , in. (mm)	θ_1 , deg	θ_2 , deg	Z/D (reference only)
1	-001	0.0591 (1.5)	65.799	62.383	5
2	-002	0.0591 (1.5)	55.828	53.232	12.5
3	-003	0.0591 (1.5)	47.750	45.334	20
4	-004	0.0787 (2.0)	63.427	60.200	5
5	-005	0.0787 (2.0)	51.140	48.942	12.5
6	-006	0.0787 (2.0)	41.984	40.534	20
7	-007	0.0984 (2.5)	61.138	58.098	5
8	-008	0.0984 (2.5)	46.980	45.128	12.5
9	-009	0.0984 (2.5)	37.247	36.154	20

power supply controller such that each phase was connected to two resistive wire elements in series.

Air was supplied to the heater through a mass flow measuring device. To achieve proper seals to prevent any leakage, gaskets were fitted to the flanges at both ends of the heater with high-temperature sealant. The temperature of the air downstream of the heater, just before the piccolo pipe, was continuously monitored throughout each test. A feedback loop using this air temperature allowed the air heater to be controlled such that a preselected air temperature in the piccolo pipe could be maintained. The mass flow of air entering the heater was measured by a calibrated Venturi meter. The mass flow of hot air impinging on the lipskin of the model has a strong influence on the heat transfer coefficients between the impinging jets and the lipskin. Therefore, it was important to measure this value accurately during the tests. This was achieved using a Venturi, which was designed and manufactured to BS1042 and calibrated with a calibrated orifice plate.

Three calibrated pressure transducers by Kulite and one by Rosemount were used for pressure measurements. The transducers were positioned along the supply pipe at three positions: upstream of the venturi, at the throat of the venturi, and just downstream of the point where the supply pipe enters the wind tunnel and on the bulkhead that formed the rear boundary of the D-chamber. The first pressure transducer was designed to measure a maximum differential pressure of 12.5 psi (86.2 kPa) in an environment with a maximum absolute pressure of 90 psia (0.621 MPa) and an extreme environmental temperature range from -54 to $+50^\circ\text{C}$.

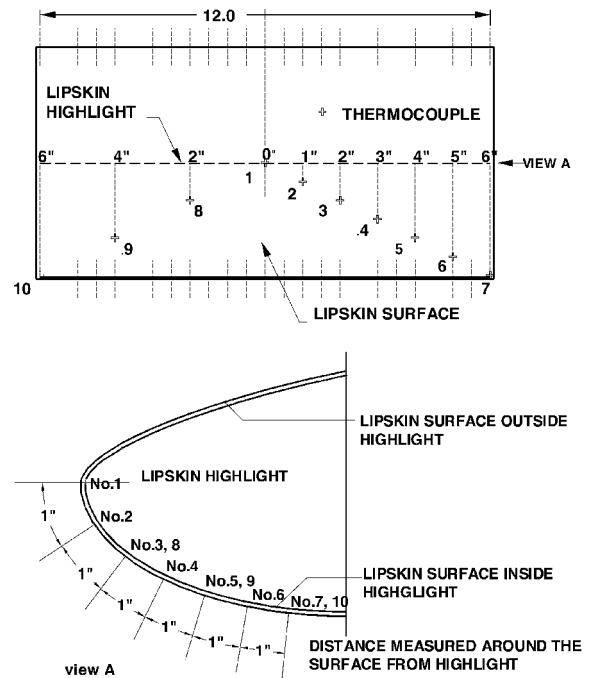
The second pressure transducer was designed to measure absolute pressure in the range 0–90 psia (0–0.621 MPa) and has the same environmental temperature limits as the first one.

The third and fourth pressure transducers were miniature, high-temperature models with absolute pressure range of 0–90 psia (0–0.621 MPa) and temperature range from -55 to $+260^\circ\text{C}$.

Four total temperature probes and 10 thermocouples were employed for temperature measurements (Fig. 5). All of the thermocouples used were K-type (nickel-chromium/nickel-aluminum), similar to those used in flight tests. The thermocouples were designed to operate in a continuous environmental temperature range of 0–1100°C. Preliminary tests were carried out to establish the accuracy of the thermocouples in measuring lipskin temperature with an external airflow. The staggered pattern of thermocouples ensured minimum interference effects of airflow over one row on another row.

Flow visualization tests with a mixture of dye and paraffin were carried out to establish that the endplates on the front D-chamber region result in the external air flow provided by the wind tunnel being uniform over the span of the model. Infrared photographs showed that the lipskin had a uniform temperature at steady-state conditions. Therefore, it may be concluded that the heat transferred from the impinging hot air jets is rapidly conducted away from the immediate impingement area and that the impingement area had a uniform heating.

The measured values of exhaust air temperature at the top and bottom of the D-chamber region are in acceptable agreement with each other giving confidence in the readings. The difference between the temperatures was within 10°C . This is important because these

**Fig. 5** Positioning of thermocouples on lipskin.

values of temperature were used to calculate the heat transferred to the lipskin.

Results and Discussion

The temperature difference between the piccolo pipe air temperature and the mean exhaust air temperature is a measure of the heat lost by the impinging air. Theoretically, the maximum temperature drop of the impinging hot jet is represented by the temperature difference between the piccolo air temperature and the adiabatic wall temperature.

The initial results presented are the value of heat lost by the impinging air based on the measured temperature difference between the piccolo air and the exhaust air. In reality some of the heat loss is not in the impingement region. The results of Hollworth and Gero,¹⁹ Gero,²⁰ and Tomich²¹ for single impinging jets were used to estimate the quantity of heat lost in this manner. The values of the average heat transfer coefficient are dependent on the area of impingement considered, and the results are corrected for an effective impingement area. The final correlation is corrected to allow for the estimated 6% heat loss, which is not transferred to the impingement region.

Figure 6 shows a typical relationship between the Reynolds number of the impinging hot airflow and the heat transfer. The results demonstrate that there is an increase in heat transfer with the increase in Reynolds number. The results shown are for three different piccolo hole patterns, each with the same hole diameter and the same pipe to lipskin separation ratio, Zn/d . It is clear from Fig. 6 that for a given value of Reynolds number, the largest heat transfer is obtained using the hole pattern with most holes and, therefore, with a minimum hole separation distance, Cx/d . It can also be observed that there is an increase in the gradient of the relationship $Nu/Pr^{1/3}$ vs Reynolds number with an increase in the number of holes. However, this improvement in heat transfer is associated with an increase in total hot air mass flow due to the increase in the number of holes. Correlations that account for the ratio of piccolo hole pitch to diameter of the form

$$\overline{Nu} = a Re^b (C_x/d)^c Pr^{1/3} \quad (1)$$

are presented in Fig. 7. The results shown represent three different hole diameters. It may be seen that, although there is a good correlation with changes in pitch for a given hole diameter, there is an increase in the value of average Nusselt number \overline{Nu} with an

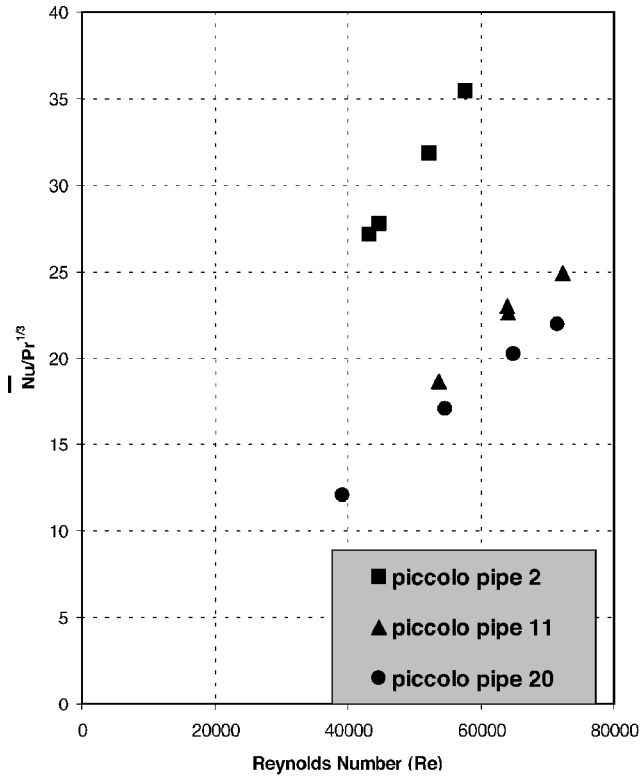


Fig. 6 Reynolds number Re vs $\overline{Nu}/Pr^{1/3}$.

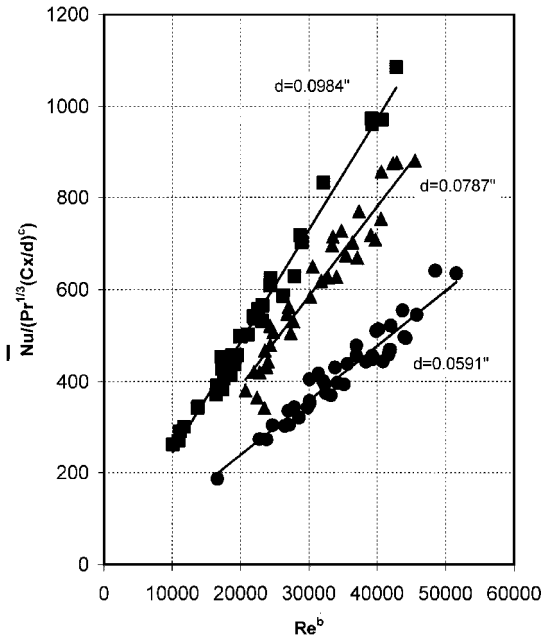


Fig. 7 Comparison of correlations for different piccolo hole diameters.

increase in the piccolo hole size. The high-pressure ratio used in the experiment ensured that the holes remain choked. Therefore, the increase in heat transfer can only be attributed to an increased mass flow of hot air without any reduction in jet velocities.

It was not possible to obtain a single relationship between average Nusselt number \overline{Nu} and Reynolds number Re based on hole diameter with all hole patterns, and this was due to the effective change in the heated impingement area for each jet produced by the changes in hole pattern. To account for this effective change in impingement area, a Reynolds number Re_G , which is based on the hot air mass

flow per unit area of impingement surface as given by the following expression, was chosen for correlation:

$$Re_G = (4/\pi)(Gd/\mu) \quad (2)$$

It is significant, as shown in Fig. 8, that the use of Re_G results in a single correlation for all pipes as follows:

$$\overline{Nu} = aRe_G^b(Cx/d)^c Pr^{1/3} \quad (3)$$

This correlation is independent of separation distance Zn/d from the impingement surface, and therefore, the effect of Zn/d over the range considered must be minimal in determining the heat transfer to the lipskin.

The effect of a variation in piccolo hole diameter on heat transfer is demonstrated in Fig. 9. The results shown here are for three different piccolo hole diameters but with the same number of piccolo holes, $N = 11$, a fixed hole separation ratio, $Cx/d = 38$, and a fixed piccolo pipe to lipskin surface separation ratio, $Zn/d = 5.0$. The

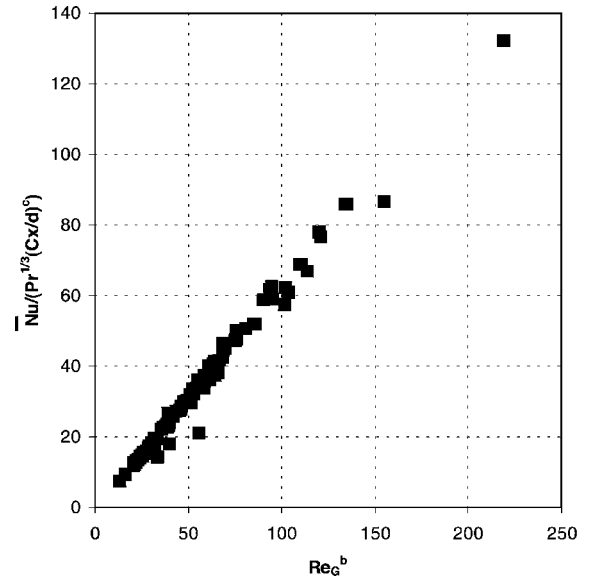


Fig. 8 Single correlation based on Re_G $\overline{Nu} = aRe_G^b(Cx/d)^c Pr^{1/3}$.

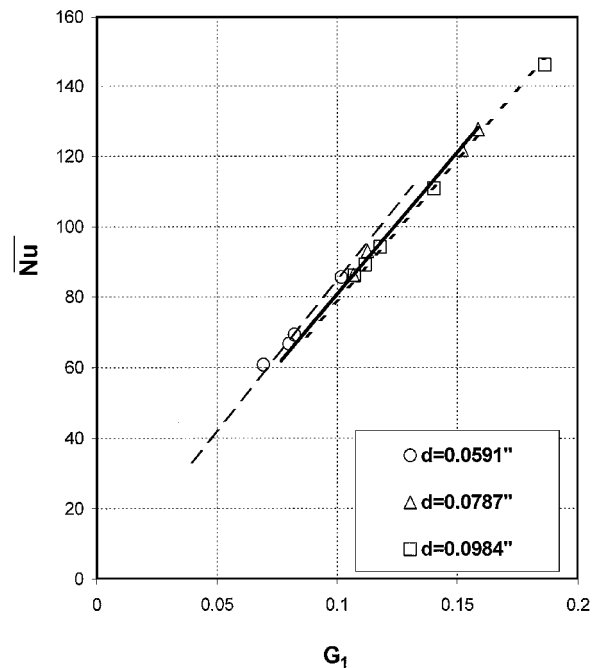


Fig. 9 Effect of piccolo hole diameter on heat transfer.

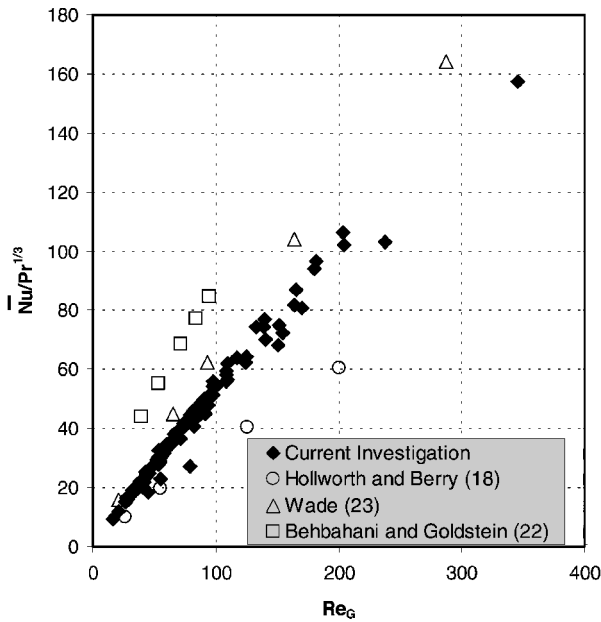


Fig. 10 Comparison of correlation with previous research.

results demonstrate that an increase in the diameter of piccolo holes results a small reduction in heat transfer coefficient. A reason for this behavior could have been that the jet exit velocity (and, hence, arrival velocity at the impingement surface) would decrease as the diameter increased. However, this would not have been possible because the holes are choked during the tests. A possible reason for this reduction of heat transfer of approximately 7–8% between the smallest and largest piccolo hole diameters is due to difference in the turbulence profiles at the exit of the holes.¹⁶ Another reason for this reduction in heat transfer could be attributed to the expansion of the jet shortly after exiting the hole. Because of the choking pressure ratio across the hole, the jet expands on exit for a short distance and attains supersonic speeds. A shock wave then occurs to return the flow to subsonic conditions. The effect on heat transfer of this shock wave and any changes in the turbulence levels associated with it is yet to be understood.

The findings of this investigation are presented along with those of three other investigators, as shown in Fig. 10. The findings of the other investigators have been arranged to be in the same format as those of the current investigation, and all investigations were carried out for arrays of circular air jets.

The correlation presented by Behbahani and Goldstein²² was constructed using results of test points for the current investigation. The following equation was applied to these results:

$$\overline{Nu} = 0.0954(4w/N\pi\mu d)^{0.78}(Zn/d)^{-0.7} \quad (4)$$

This is adapted from Ref. 22, for values of jet exit to surface separation ratio, $Zn/d = 5$.

Wade²³ has provided sufficient information concerning the system geometry and testing flows such that values of Re_G and average Nusselt number could be calculated for test points contained therein. Test points with a cooling airflow velocity of 47.9 m/s were chosen. Therefore, the correlation presented by Wade²³ has been derived from results, which are unrelated to the current investigation.

The results of Behbahani and Goldstein²² are shown to have the greatest value of average heat transfer coefficient for a given value of Re_G . The current investigation along with that of Wade²³ employed arrays of jets that included angles of impingement less than 90 deg, that is, $\theta < 90$ deg. As discussed earlier, Sparrow and Lovell¹¹ demonstrated that the average heat transfer coefficient is reduced at angles of impingement less than 90 deg. Therefore, we would expect greater heat transfer in the experiments of Behbahani and Goldstein²² in which all jets impinge normally to the target surface.

The resulting correlation of Hollworth and Berry¹⁷ was also obtained from experiments using impingement angles of 90 deg, and therefore, we might expect levels of heat transfer similar to those found by Behbahani and Goldstein.²² However, although the values of Re_G are similar, this value is not indicative of a similar flow from the holes because the area of the hole is no longer a variable in the calculation of Re_G . Therefore, the jet velocities in the experiments of Hollworth and Berry,¹⁷ which were very low compared to the current investigation, do not necessarily result in a low value of Re_G as they would have done using Reynolds number Re . These low exit velocities result in low values of heat transfer, which is demonstrated in Fig. 9.

The correlation that lies closest to the result for the current investigation is that of Wade.²³ This is to be expected, perhaps, because the system is very similar to the current investigation. Indeed, the two systems are so similar that the question of why the two correlations are not closer arises. This may simply be explained by experimental errors between the two sets of results. For the current investigation, the maximum error in the measurement of the average Nusselt number is $\pm 15\%$. This is likely to be an explanation in part. There are differences in the exhaust air geometry to that of Wade,²³ which has a castellated ring at the bottom of the front bulkhead. This would lead to a different flow pattern within the D-chamber region resulting in differing crossflow effects that may affect heat transfer to the lipskin.

Although the hole diameters are similar, differences in the manufacturing process may mean that the holes have sharper edges. This would affect the inlet turbulence levels, which have been demonstrated by Obot et al.¹⁶ to affect the velocity and turbulence profiles of the jet at the hole exit.

Under steady-state conditions, the lipskin temperature is such that there is equilibrium between heat flow from the hot air jets on the internal surface and heat flow to the cooling external airflow. The external cooling air velocities for the test cases used to generate the correlation from the work of Wade²³ are 20% greater than those generated in the current investigation. In addition, the heat balance calculated by Wade²³ is based on predicted values of external heat transfer coefficient, which are used in the determination of the amount of heat flow. The calculated values of heat transfer in the current investigation were based on the measured temperature drop of the impinging hot air. A combination of these reasons probably explains the differences in the correlation of Wade²³ and the current investigation.

Conclusions

The following conclusions can be drawn from the results of the present investigations.

To optimize the heat transfer, the smallest hole diameter that will be sufficient to pass the required mass flow should be used. This will not only result in increased heat transfer due to the effect of the hole diameter but will also ensure that a reduction in heat transfer performance for a separation ratio greater than 5 will not occur.

The use of a Reynolds number for the flow that is based solely on hole diameter and does not take into account the area of the impingement surface will not lead to a single correlation relating heat transfer. The heat transfer to the jet impingement region for a system with three rows of jets may be predicted with reasonable accuracy using a Reynolds number based on unit area of impingement surface as given by following relationship:

$$\overline{Nu} = aRe_G^b(C_x/d)^cPr^{\frac{1}{3}} \quad (5)$$

Additional heat transfer processes occurring in multiple jet impingement may be due to turbulence produced by wall jet interaction.

References

- Sogin, H. H., "A Design Manual for Thermal Anti-Icing Systems," WADC TR 54-313, Wright Air Development Center, Wright-Patterson AFB, OH, Dec. 1954.
- Gaunter, J. W., Livingood, J. N. B., and Hrycak, P., "Survey of Literature on Flow Characteristics of a Single Turbulent Jet Impinging on a Flat Plate," NASA TN D-5652, 1970.

- ³Hrycak, P., "Heat Transfer from Impinging Jets. A Literature Review," AFWAL-TR-81-3054, Air Force Wright Aeronautical Labs., June 1981.
- ⁴Gardon, R., and Cobonpue, J., "Heat Transfer Between a Flat Plate and Jets of Air Impinging on It," *International Heat Transfer Conference*, Pt. 2, 1961, pp. 454-460.
- ⁵Hrycak, P., Jachna, S., and Lee, D. T., "A Study of Characteristics of Developing Incompressible, Axisymmetric Jets," *Letters in Heat and Mass Transfer*, Vol. 1, 1974, pp. 67-72.
- ⁶Gardon, R., and Akfirat, J. C., "The Role of Turbulence in Determining the Heat Transfer Characteristics of Impinging Jets," *International Journal of Heat and Mass Transfer*, Vol. 8, 1965, pp. 1261-1272.
- ⁷Hrycak, P., Lee, D. T., Gaunter, J. W., and Livingood, J. N. B., "Experimental Flow Characteristics of a Single Turbulent Jet Impinging on a Flat Plate," NASA TN D-5690, 1970.
- ⁸Huang, L., and El-Genk, M. S., "Heat Transfer of an Impinging Jet on a Flat Surface," *International Journal of Heat and Mass Transfer*, Vol. 37, No. 13, 1994, pp. 1915-1923.
- ⁹Metzger, D. E., Yamashita, T., and Jenkins, C. W., "Impingement Cooling of Concave Surfaces with High Velocity Impinging Air Jets," *Journal of Engineering for Power*, Vol. 91, 1969, pp. 149-158.
- ¹⁰Perry, K. P., "Heat Transfer by Convection from a Hot Gas Jet to a Plane Surface," *Proceedings of the Institute of Mechanical Engineers*, London, Vol. 168, 1954, pp. 775-780.
- ¹¹Sparrow, E. M., and Lovell, B. J., "Heat Transfer Characteristics of an Obliquely Impinging Circular Jet," *Journal of Heat Transfer*, Vol. 102, May 1980, pp. 202-209.
- ¹²Martin, H., "Heat and Mass Transfer Between Impinging Gas Jets and Solid Surfaces," *Advances in Heat Transfer*, Vol. 13, Academic Press, New York, 1977, pp. 1-60.
- ¹³Hollworth, B. R., and Bowley, W. W., "Heat Transfer Characteristics of an Impinging Jet in a Crossflow," American Society of Mechanical Engineers, ASME Paper 75-WA/HT-100, Nov.-Dec. 1975.
- ¹⁴Colin, P. E., and Olivari, D., "The Impingement of a Circular Jet Normal to a Flat Surface With and Without Crossflow," Von Kármán Inst. for Fluid Dynamics, TR 1, 1969.
- ¹⁵Sparrow, E. M., Goldstein, R. J., and Rouf, M. A., "Effect of Nozzle-Surface Separation Distance on Impingement Heat Transfer for a Jet in a Crossflow," *Journal of Heat Transfer*, Nov. 1975, pp. 528-533.
- ¹⁶Obot, N. T., Majumdar, A. S., and Douglas, W. J. M., "The Effect of Nozzle Geometry on Impingement Heat Transfer Under a Round Turbulent Jet," American Society of Mechanical Engineers, ASME Paper 79-WA/HT-53, 1979.
- ¹⁷Hollworth, B. R., and Berry, R. D., "Heat Transfer from Arrays of Impinging Jets with Large Jet-to-Jet Spacing," American Society of Mechanical Engineers, ASME Paper 78-GT-117, 1978.
- ¹⁸Metzger, D. E., "Spot Cooling and Heating of Surfaces with High Velocity Impinging Air Jets," TR 52, Dept. of Mechanical Engineering, Stanford Univ., Stanford, CA, 1962.
- ¹⁹Hollworth, B. R., and Gero, L. R., "Entrainment Effects on Impingement Heat Transfer: Part II—Local Heat Transfer Measurements," *Journal of Heat Transfer*, Vol. 107, Nov. 1985, pp. 910-915.
- ²⁰Gero, L. R., "Heat Transfer from a Non-Isothermal Impinging Jet," M.S. Thesis, Mechanical and Industrial Engineering Dept., Clarkson College of Technology, Potsdam, NY, Oct. 1983.
- ²¹Tomich, J. F., "Heat and Momentum Transfer from Compressible Turbulent Jets of Hot Air Impinging Normally to a Surface," Ph.D. Dissertation, Sever Inst. of Technology, Washington Univ., Saint Louis, MO, Jan. 1967.
- ²²Behbahani, and Goldstein, "Local Heat Transfer to Staggered Arrays of Impinging Circular Air Jets," American Society of Mechanical Engineers, ASME Paper 82-GT-211, 1982.
- ²³Wade, S. J., "Modelling of the Performance of a Thermal Anti-Icing System for Use on Aero-Engine Intakes," M.Sc. Thesis, Dept. of Mechanical Engineering, Loughborough Univ. of Technology, Loughborough, England, U.K., Nov. 1986.